Article

High Temperature Microtribological Studies of MoS$_2$ Lubrication for Low Earth Orbit

Peter Serles [1], **Khaled Gaber [1]**, **Simo Pajovic [1,2]**, **Guillaume Colas [3]** and **Tobin Filleter [1,*]**

[1] Department of Mechanical & Industrial Engineering, The University of Toronto, 5 King's College Road, Toronto, ON M5S 3G8, Canada; pserles@mie.utoronto.ca (P.S.); khaled.gaber@mail.utoronto.ca (K.G.); simo.pajovic@mail.utoronto.ca (S.P.)

[2] Department of Mechanical Engineering, Massachusetts Institute of Technology, 77 Massachusetts Ave, Cambridge, MA 02139, USA

[3] Department of Applied Mechanics, Université Bourgogne Franche-Comté FEMTO-ST Institute CNRS/UFC/ENSMM/UTBM, 24 rue de l'Epitaphe, F-25000 Besançon, France; guillaume.colas@femto-st.fr

* Correspondence: filleter@mie.utoronto.ca

check for updates

Abstract: Molybdenum disulfide is one of the most common lubricant coatings for space systems but it displays enormous susceptibility to environmental conditions making it hard to predict performance throughout the entire lifetime. The majority of mechanisms for space operate in low Earth orbit where temperatures typically reach 120 °C along with exposure to highly reactive atomic oxygen which can be detrimental to lubricant performance. In the present study, a MoS$_2$ lubricant coating is tested using friction force microscopy under different environmental conditions including air and dry nitrogen environments with temperatures ranging from 25 °C to 120 °C. The increased temperature was found to be beneficial for friction behaviour in air up to 100 °C as ambient humidity is removed from the contact, but higher temperatures become detrimental as increased reactivity leads to oxidation. These competing effects resulted in a minimum coefficient of friction at 110 °C in the air environment. The high temperature also increases the wear of the coatings as the intrinsic shear strength decreases with thermal energy which in turn disrupts tribofilm formation leading to increased friction. The run-in duration and magnitude are both found to decrease with temperature as the energy barrier to optimal reconfiguration is reduced. Finally, contextualization of the present findings for mechanisms operating in low earth orbit is discussed.

Keywords: molybdenum disulfide; friction force microscopy; low earth orbit; space lubrication; temperature; tribology

1. Introduction

Friction and wear of space systems is a multifaceted problem facing extreme conditions rarely encountered or engineered for on Earth. Low gravity, extreme operating temperatures, radiation, and inability to easily perform maintenance are among the basic challenges which all contribute to the collective difficulty in providing long-lasting and predictable lubrication for space systems [1]. Lubrication for space takes three main forms: liquid (predominantly synthetic oils), grease (liquid lubricants with a thickener), or solid (materials with low interfacial shear strength and surface energy) [2]. Each lubrication method has its own respective strengths and weaknesses but solid lubricants have become increasingly attractive for spacecraft as they don't suffer from contact creep [3] or vacuum outgassing [4] and offer excellent thermal stability [5]. Thermal stability and durability in vacuum are two of the most prominent advantages of solid lubricant coatings and are especially favourable for the dominant space-qualified solid lubricant, molybdenum disulfide (MoS$_2$).

MoS_2 has been studied as a lubricant for space and vacuum applications since the 1940s [6] due to its atomic 2D lamellar structure which provides an extremely low interfacial shear strength. MoS_2 thrives in conditions that are free of humidity making it an excellent lubricant for vacuum and it offers thermal stability up to 1200 °C [7,8]. However, a majority of space systems operate within a distinct range of conditions in the Low Earth Orbit (LEO) atmosphere which consists of a high vacuum environment (~10^{-8} Pa [9]) with reactive atomic elements (O^{2-}, H^+, He^-) as well as a wide range of often cyclic temperatures (±120 °C) [4,10]. Oxidation of MoS_2 is common in humid or oxygen-rich environments such as LEO (~10^9 O^{2-} cm^{-3} representing 96% of atomic exposure at 400 km orbit) [11,12] which leads to the breakdown of lubricating properties following the formation of MoO_3 and MoS_xO_y [13–15]. The resulting MoS_xO_y stoichiometry is proportional to the exposure time and incidence of reactive oxygen [16] and prolonged exposure has demonstrated increased wear and friction behaviour for MoS_2 coatings [14,17]. MoS_2 lubricants which have been exposed to the LEO atmosphere from the international space station have shown significant oxidation and degraded microtribological behaviour in as little as 43.5 h [13,18]. However, MoS_2 lubrication under increased temperatures in terrestrial environments have shown decreasing coefficient of friction in temperatures up to 100 °C [19] but both increasing friction and wear above 100 °C [20,21]. The contributions of thermal energy as well as oxygen reactivity are both detrimental to the tribological performance, however, understanding the underlying mechanistic impact of these tribochemical effects on the friction and wear performance remains limited.

In the present study, a high-resolution microtribological analysis of a space-qualified MoS_2 coating with increasing temperature is performed using friction force microscopy (FFM) customized with space-grade AISI 440C steel contacts. The steel on MoS_2 contact presents identical tribochemical conditions to typical bearing and gear systems used in space [22,23], while FFM allows for nanometer-resolution in measuring in situ wear and friction evolution. The FFM configuration used has been outfitted with a customized environmental control box (ECB) allowing for controlled temperature and humidity conditions within the local environment. The ultimate reliability of spacecraft within LEO will depend on the durability of moving systems throughout a range of temperatures and environments. Ensuring predictable performance requires operational knowledge throughout all atypical conditions that a system might face including those evaluated herein.

2. Materials and Methods

2.1. MoS₂ Solid Lubricant Coating

A 1 μm thick MoS_2 coating has been prepared by direct current-magnetron sputter deposition and deposited on an N-doped (100) silicon wafer with a 285 nm SiO_2 top layer. The coating was deposited using a space-qualified deposition process by Teer Coatings Ltd. (Droitwich, UK) and includes a 200 nm adhesion layer of MoS_2 + titanium as seen in Figure 1a. Figure 1b shows a high resolution transmission electron microscope (HRTEM, Hitachi Ltd., Tokyo, Japan) image of the cross-sectional crystal structure and Figure 1c depicts the selected area electron diffraction (SAED) pattern. The coating consists of a mean crystal size of 6 nm with texture in the (002) noted in the SAED pattern. The corresponding molecular structure of MoS_2 is schematised in Figure 1d with the "deck of cards" shearing effect under tribological loading. The cross-sectional TEM samples were prepared using the Focused Ion Beam (FIB) lift-out method. The sample was thinned to <80 nm using FIB after the application of a tungsten protection layer (Figure 1a).
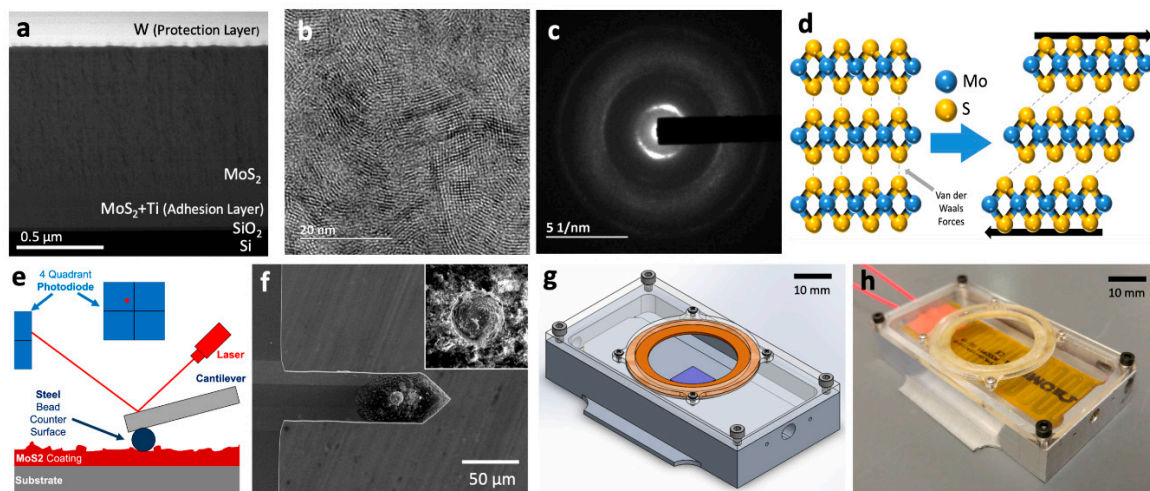
Figure 1. (**a**) Dark field STEM image of the entire coating including the FIB-protection layer; (**b**) HRTEM image of the MoS$_2$ nanocrystalline structure; (**c**) SAED pattern of the MoS$_2$ coating showing nanocrystalline rings with texture; (**d**) Molecular structure of MoS$_2$ demonstrating van der Waals sliding when subjected to shear forces; (**e**) FFM schematic of steel bead the MoS$_2$ coating; (**f**) Custom-made AFM cantilevers with AISI 440c steel bead contact, inset of the bead after use; (**g**) SolidWorks isometric projection of the ECB; (**h**) Photo of the finished ECB for AFM.

2.2. Friction Force Microscopy

FFM was performed using an Asylum MFP-3D Atomic Force Microscope (AFM, Asylum Research; Oxford Instruments, Goleta, CA, USA) outfitted with custom-made AFM cantilevers as schematized in Figure 1e. The AFM cantilevers were prepared by attaching a ~10 μm diameter AISI 440c stainless steel bead (Sandvik Osprey Ltd., Neath, UK) to NANOSENSORS Tipless Silicon cantilevers (NanoSensors Inc., Neuchâtel, Switzerland) of 60 ± 8 N/m stiffness (Figure 1f). The normal force was determined to correspond to 1 GPa contact pressure with normal loads of 30-35 μN [24], the contact length was 60 μm, and the contact velocity was set to 0.25 Hz or 15 μm/s. The tests were carried out to a total of 1024 cycles with 1024 data points per line (every 58 nm travelled). The cantilever normal [25] and lateral [26] stiffness calibration was performed as per the respective Sader methods and lateral sensitivity as per the test probe method [27]. The normal stiffness was doubled to account for the trapezoidal geometry of the cantilever. The coating surface was first imaged in tapping mode to find an area free of debris and damage, after which the cantilever was positioned for a 60 μm long, single-wide wear track in reciprocating linear contact. The normal force was held constant and the normal deflection and bi-directional lateral deflection signals were recorded. The cantilevers were cleaned between each test to remove wear debris particulate by AFM-driven vibration in acetone and ethanol for 10 min each.

2.3. Environmental Control for FFM

A custom-designed environmental control box was manufactured and outfitted to the Asylum MFP-3D AFM as seen in Figure 1g,h. The ECB allows sealed sample access for the AFM with ambient environmental control through inflowing gas and local resistive heating of the sample. The gas inflow was fed through a porous polyurethane foam diffuser to avoid sample or cantilever disruption and the sample stage was rigidly secured to the box. An ambient humidity and temperature sensor was installed in the box and sealed. Air tests were performed at 28–36% RH based on the ambient environment and nitrogen tests were performed at <2% RH following 30 min of chamber purging at 5 standard cubic feet per hour (SCFH) with 99.99% pure N$_2$. Throughout nitrogen tests, a constant inflow of nitrogen gas at 2 SCFH was maintained to ensure positive internal pressure. The resistive heating was provided by a 10 W/in^2 polyimide film flexible heater (KHLVA-101/10-P, OMEGA Engineering, Norwalk, CN, USA) and controlled via an Arduino open-loop temperature controller. An additional off-the-shelf

temperature controller (SL4824-VR-D, AutomationDirect, Atlanta, GA, USA) was used to shut the heater off in case of emergency (i.e., the exterior temperature of the box becoming damaging to the AFM). Temperature was measured using two type K thermocouples (OMEGA Engineering, SA1-K-72). The heating stage was suspended rigidly in the box and insulated on five sides with polyurethane foam. The sample temperature was allowed to stabilize for 30 min prior to testing and the AFM cantilever was placed into contact during temperature stabilization to account for any thermal expansion of the cantilever. The ECB was designed and iterated to provide consistent and controllable localized temperature and environmental control; details of the ECB design are included in Figure SI1.

3. Results & Discussion

3.1. Friction Behaviour

The MoS_2 coating was subjected to at least four 1024-cycle FFM tests for each of the ten conditions. Seven temperatures ranging from 25 °C to 120 °C for ambient air environments and three temperatures for inert nitrogen environments were studied. The average coefficient of friction as a function of temperature for the steady-state friction cycles (cycles 100–1024) is shown in Figure 2a. For the tests in air, the friction is found to decrease with respect to temperature until 110 °C and begin to increase again at 120 °C. This effect is characteristic of MoS_2 tribological contacts at elevated temperatures when ambient humidity is present [28,29]; the ambient humidity allows water intercalation between 2D MoS_2 sheets [30,31] which hinders the van der Waals sliding and increases the interfacial shear strength. As temperature increases, the desorption of water from the contact increases and the MoS_2 has reduced resistance to shear. Additionally, increased thermal energy in the system is believed to be the primary cause of oxide formation. Raising the system temperature from 25 °C to 150 °C has shown surface oxidation of Mo to MoO_3 from 20% to 95% [32]. Two competing mechanisms are therefore at play throughout this temperature range: higher temperatures promote desorption of water species which decreases friction in MoS_2 coatings but also promotes the oxidation of MoO_3 which increases friction. The critical temperature of 110 °C therefore suggests an optimal balance between these two competing mechanisms and results in the minimum friction in humid air.

Friction tests were additionally performed under inert nitrogen conditions to isolate thermal and tribochemical effects. At room temperature, the friction coefficient under nitrogen is significantly lower than that of the air environment at $\mu_{N2} = 0.062 \pm 0.002$ compared to $\mu_{Air} = 0.45 \pm 0.02$. However, despite eliminating the tribochemical effects of oxidation and water desorption in the inert nitrogen environment, the friction is found to increase to $\mu = 0.094 \pm 0.007$ at 100 °C and $\mu = 0.086 \pm 0.005$ at 120 °C. Similar increase of friction with higher temperature for MoS_2 coatings under inert N_2 and vacuum environments have been previously demonstrated [28,29,33], however, little discussion of the mechanisms for increasing friction under oxidation-free environments have been explored.

This increased friction as a result of increasing temperature is contrary to the intrinsic tribological characteristics for high-temperature MoS_2 contacts; Curry et al. [34] reported decreasing shear strength with increasing temperature for 2D MoS_2 simulations attributed to the lower external energy barrier for incommensurate sliding. This lowered shear strength results in a lower coefficient of friction as the MoS_2 van der Waals layers provide less resistance to sliding. Additionally, the lattice spacing of MoS_2 increases with respect to temperature [35], as would be expected by thermal expansion, which further decreases the intrinsic resistance to shear. However, both these mechanisms only account for the internal shear mechanisms of MoS_2 and do not account for the entirety of the tribological contact. The decreased shear strength and increased lattice spacing also result in an increased wear rate as the van der Waals layers are easier to cleave [34]. Increased wear rates at higher temperatures of MoS_2 coatings under vacuum have been identified experimentally and also demonstrated increasing mean wear particle size with temperature [36]. This suggests that MoS_2 coatings operating in the wear regime at high temperature are susceptible to a number of different tribological mechanisms concurrently.
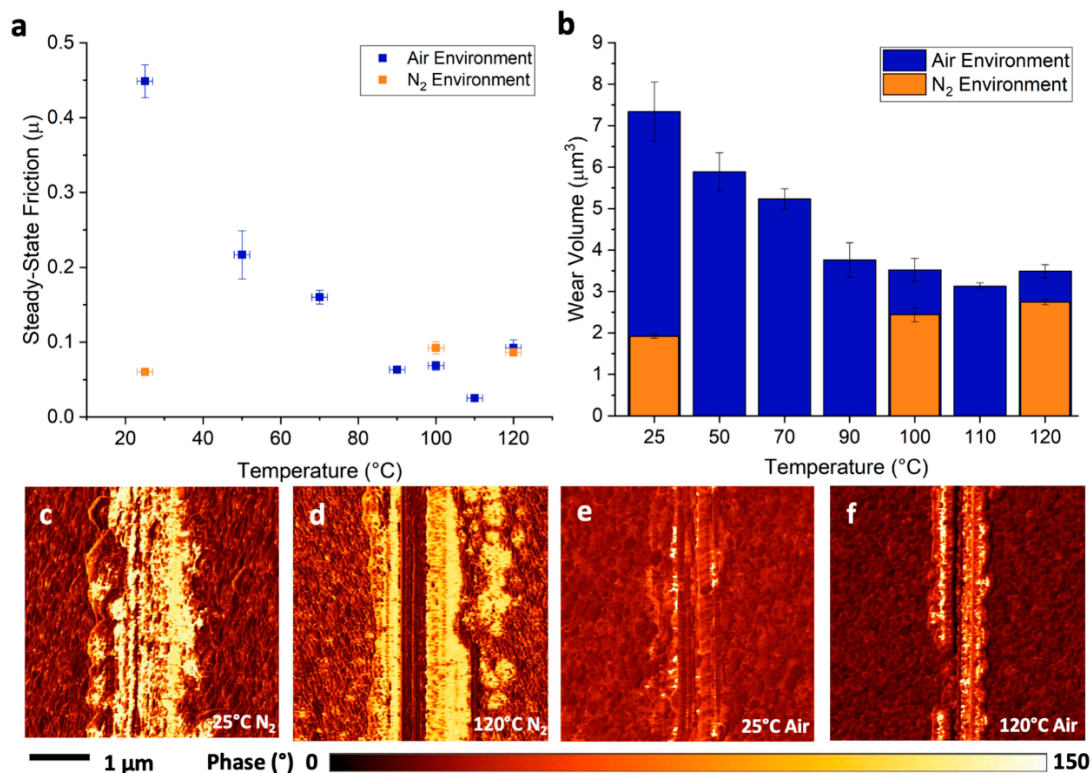
Figure 2. (**a**) Average steady-state (cycle 100–1024) coefficient of friction for the various temperatures and environments, Y error bars show standard deviation from 924 cycles and N > 3 test; (**b**) Total wear volume after 1024 cycles for each test; AFM tapping mode phase image of the wear track following 1024 cycles for tests in (**c**) 25 °C nitrogen, (**d**) 120 °C nitrogen, (**e**) 25 °C air, (**f**) 120 °C Air; Lateral 1 μm scale bar and Phase 0–150° scale bar below.

3.2. Wear Mechanics

The total wear volume for the ten different environmental conditions is presented in Figure 2b. This wear volume is calculated as a function of the penetration depth of the steel bead into the MoS_2 coating. The AFM change in height is measured during FFM and the steel bead volume is imaged to determine the total wear volume [24]. The difference between air and nitrogen environments is immediately apparent as even the lowest wear volume for any air environment ($V_{Air, 110 °C} = 3.13 \pm 0.08 \mu m^3$) is still greater than the largest wear volume for any nitrogen environment ($V_{N2, 120 °C} = 2.65 \pm 0.07 \ \mu m^3$). This contrast is most apparent at room temperature where the wear volume under air environments is more than 350% that of the nitrogen environment meanwhile at higher temperatures the difference in wear volume drops to ~130%. As the lower temperatures are dominated by water intercalation effects, this suggests a significant mechanism for weakening the inter-layer bonding and increasing wear; Levita et al. [31] calculated the equilibrium spacing of MoS_2 layers to increase from 3.07 Å to 4.53 Å following water intercalation. However, in the present bulk samples, this spacing may not be possible due to confinement which would in turn create significant internal stresses that would also reduce the shear strength and promote wear.

At higher temperatures above 90 °C, the wear volume in air becomes fairly consistent which likely results from the complete desorption of water and transition to higher temperature wear mechanisms, including increased surface oxidation and decreasing shear strength. The tests in air continue to present higher wear rates than the nitrogen environment due to this contribution of oxide formation as well as the intrinsic thermal effects. The tests in nitrogen environments, without the effect of oxidation or humidity, nonetheless show increased wear rates with increasing temperature which agrees with the thermal energy decreasing shear strength. The wear volume is indeed found to further increase

slightly between 100 °C and 120 °C ($V_{N2,100\,°C}$ = 2.44 ± 0.17, $V_{N2,120\,°C}$ = 2.75 ± 0.07) despite statistically similar values for steady state friction. This is in agreement with other reports of wear rates for MoS_2 at high temperature in inert environments [36,37].

As previously mentioned, the increasing friction at higher temperatures in inert environments is contrary to the decreased intrinsic shear strength resulting from increased thermal energy. This suggests that additional mechanisms are disrupting the tribological contact to increase the friction. The high temperature wear characteristics are likely a major contribution to disrupting the tribological surface contact for two reasons: 1. contacts with higher wear have a reduced likelihood of forming a stable lubricating tribofilm on the surface as it is continually worn off; 2. it has been noted that the mean wear particle size increases with temperature [36], which would result in a surface of increased surface roughness and disrupt the contact.

To investigate further, AFM tapping mode phase imaging of the wear tracks were performed after the 1024 cycle tests and representative profiles for 25 °C and 120 °C are presented for both environments in Figure 2c–f. Phase imaging detects changes in the adhesion and stiffness of the surface material through AFM tapping mode contact and is therefore commonly used to identify tribofilm formation through contrasting phase [38,39]. It can be seen that of the four environments shown, only the room temperature test in a nitrogen environment truly forms a complete and cohesive tribofilm throughout the entire contact (Figure 2c). The tests at elevated temperature in nitrogen (Figure 2d) show the majority of the wear track forming a tribofilm but a significant wear scar exposing the underlying MoS_2 in the middle of the track. This suggests a more complex tribological contact with increased temperature where the greater intrinsic wear rate leads to stripping of the surface tribofilm underneath the contact. Conversely, for the two tests in air (Figure 2e,f) there exist a slight tribofilm within the contact but with much of the wear scar showing the underlying MoS_2 coating.

The humidity and oxidation effects due to operation in the air environment are both surface effects which would lead to continual removal of any surface tribofilm formation exposing the underlying coating as seen. The tribofilms in air do however appear to have greater coverage at higher temperatures which suggests that humidity is a larger detriment than oxidation towards tribofilm formation. However, it can be seen in Figure 2f that a section of tribofilm about 1.5 μm long has worn off which demonstrates brittle surface wear. The tribofilm is indicative of the surface evolution but it should be noted that while the wear scars for 120 °C N_2 and 25 °C air both similarly show the underlying coating rather than the protective tribofilm, the coefficient of friction is drastically different. This is due to the other surface tribological factors such as tribochemical reactivity and meniscus formation. While intrinsic friction within the MoS_2 coating should decrease with increasing temperature, it is clear that the overall performance of the coating in the wear regime is due to several different complex mechanisms working concurrently. As such, the higher wear rate as a result of temperature leads to detrimental surface effects and an increased coefficient of friction as seen herein.

3.3. Run-in Characteristics

High temperature operation can promote wear and be detrimental to the total service life of a lubricant coating, but the increased wear can also have a beneficial effect. Solid lubricant coatings have a characteristic "run-in" phase where the contact is smoothed, any oxide layers are worn off, and the tribofilm begins to form [40]. This phase is typically associated with higher friction which stabilizes after 10–100 cycles depending on the contact conditions. For space applications, run-in can be a difficulty as lubricated mechanisms in space are without maintenance and entirely remotely controlled so predictability and consistent performance throughout their lifetime is critical. This is especially difficult for single-use mechanisms such as the opening of solar panels on a satellite where the initially higher friction may cause deployment issues. Figure 3a,b show the per-cycle coefficient of friction for the various temperatures and environments averaged from a minimum of four tests per condition. For all the tested environments, the first 20–80 cycles present higher friction coefficients during the run-in phase compared to steady-state operation (cycles 100–1024). The duration of this

run-in phase as a function of environment is presented in Figure 3c where the "cycles to run-in" is determined based on the friction curve converging with its own linear fit for steady-state operation. Additionally, the magnitude of run-in is presented in Figure 3d and is defined as the difference between the friction coefficient for cycle 1 and the steady state friction.
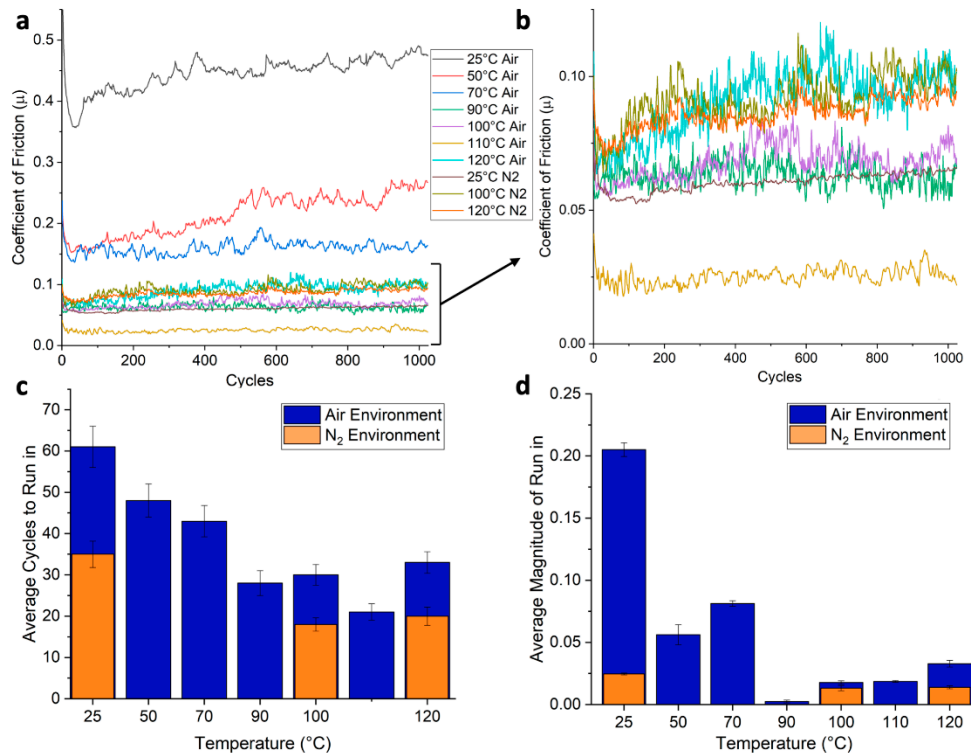

Figure 3. (**a**) Coefficient of friction evolution with respect to cycle number for the various temperatures and environments; (**b**) Coefficient of friction evolution with truncated Y axis to highlight differences; (**c**) Average number of run-in cycles until steady-state behaviour begins for each configuration; (**d**) Average magnitude of coefficient of friction decrease between the first friction cycle and the steady-state average.

The cycles to run-in decrease with increasing temperature for both air and nitrogen environments. This suggests that the increased thermal energy is able to help the coating more rapidly reconfigure for optimal tribological contact. This is likely due to a combination of factors including greater surface wear for oxidation removal, rapid surface smoothing through wear, or decreased energy barriers for sub-surface reorientation and crystallization [35,41,42]. It should be noted that while the run-in duration would logically decrease with the magnitude of friction, it is found to decrease with temperature in the N_2 environment despite the coefficient of friction increasing. Additionally, instability of the system may suggest a longer time to achieve stable steady state friction but the standard deviation for steady state friction shows no correlation with the run-in duration (cf. Table SI2). The magnitude of run-in also decreases with temperature further suggesting the enhanced ability for the coating to reconfigure and reach its steady-state operation with the aid of thermal energy. This is especially important for the predictability and control of space systems as the majority of operation may occur before steady-state operation for certain mechanisms.

Finally, the behaviour of 25 °C and 50 °C tests in air present increasing trends throughout the duration of the test while others present near-flat trends (cf. Figure 3a). This increasing friction suggests an inability to form a smooth, controlled, and sustainable friction contact in these environments which is in agreement with the lack of tribofilm observed in Figure 2e. The ambient humidity at low

temperatures is therefore completely detrimental to the performance of this MoS_2 coating and both increases the coefficient of friction and inhibits stable friction operation.

3.4. Implication for Mechanisms in LEO

The ten selected ambient conditions for the tribological tests were selected to explore the temperature range expected in low earth orbit and determine the effect of environmental species at these temperatures. While the high temperature range expected for LEO only extends to 120 °C, it is seen that this temperature is enough to create a significant change in the tribological contact. Vacuum conditions are expected in LEO however the abundance of highly reactive atomic oxygen would produce significant oxidation within the contact which, as noted for high temperature air environments, increases both the friction and wear behaviour of the coating. This additionally creates a tribofilm which is fragile and susceptible to removal by surface wear along the oxide layer. Therefore, limiting the exposure of the coating to the ambient LEO environment would be beneficial and the current research direction to create environmentally resistant MoS_2 coatings by co-deposition [43] is applicable to LEO operation as well as terrestrial conditions.

The increased temperature contributes to increased surface oxidation but, even without oxidation, the friction is found to increase at higher temperatures due to the complexity of the wear contact. However, the increased temperature is also found to be advantageous for certain tribological characteristics. The duration of run-in is found to decrease with temperature for both oxygen-rich and inert environments suggesting the thermal energy promotes easier reconfiguration of the coating for long-term tribological contact. Therefore, initial operation of a mechanism can be better controlled and predicted through operation at high temperatures as the unpredictable run-in phase is shortened. As well, the magnitude of run-in decreases with temperature meaning the friction on the first cycle is lowered with increasing temperature. This is especially important for single-use mechanisms such as the deployment of solar panels for satellites and spacecraft. It is therefore possible to optimize when this deployment occurs based on the ambient temperature with the magnitude of initial friction decreasing based on temperature.

4. Conclusions

MoS_2 has been used as a lubricant for space for over sixty years and yet due to the vast range of environmental conditions in which the lubricant operates, significant unpredictability still occurs in space mechanisms [44,45]. As low Earth orbit represents the operating conditions for the vast majority of components which are launched into space [9], this environment requires careful study and consideration for lubricants designed for space components. It is seen in the present study that the role of humidity and oxygen are both detrimental to the performance of MoS_2 friction and wear lives. Humidity is most detrimental at lower temperatures but has reduced influence above the water desorption temperature of 90–100 °C while oxidation increases with temperature due to increased reactivity. Both of these effects lead to increased surface wear and therefore difficulty for the coating to form a stable tribofilm. This increases the coefficient of friction in the contact and inhibits the lubricating ability of the coating.

To isolate the effect of increased thermal energy from the surface chemical effects, the lubricant was also tested in inert nitrogen environments. It was found that the wear and friction both increased with temperature through the 120 °C range. The increasing friction is contrary to the intrinsic material properties of MoS_2 at high temperature but is instead attributed to the increased complexity of the tribological contact when the coating operates in the wear regime. The increased thermal energy additionally plays a role in decreasing both the duration and magnitude of the run-in phase helping to accelerate the transition to predictable steady-state operation. Several different factors of MoS_2 solid lubrication are shown to be affected by increased thermal energy in LEO conditions. This leads to a lubricant contact that requires additional care for end-use application but with the potential for optimization for specific mechanisms operating in LEO.

References

1. Roberts, E.W. Space tribology: Its role in spacecraft mechanisms. *J. Phys. D Appl. Phys.* **2012**, *45*, 305001. [CrossRef]

2. Fusaro, R.L. Lubrication of Space Systems. In Proceedings of the Society of Tribologists and Lubrication Engineers Annual Meeting, Pittsburgh, PA, USA, 1994; Available online: https://ntrs.nasa.gov/search.jsp?R=19940024896 (accessed on 21 April 2020).

3. Fusaro, R.L.; Khonsari, M.M. *Liquid Lubrication for Space Applications*; NASA: Hanover, MD, USA, 1993.

4. Antoniazzi, J.; Milligan, D. A Review of Lubrication on the Canadarm 2. In *Protection of Materials and Structures from Space Environment*; Springer: Berlin, Germany, 2004; pp. 291–298.

5. Jones, W.; Jansen, M. Lubrication for Space Applications. *Handb. Lubr. Tribol.* **2010**, *222*, 997–1004.

6. Godfrey, D.; Nelson, E. *Oxidation Characteristics of Molybdenum Disulfide and Effect of Such Oxidation on its Role as a Solid-Film Lubricant*; National Advisory Committee for Aeronautics, 1949. Available online: https://ntrs.nasa.gov/search.jsp?R=19930082560 (accessed on 21 April 2020).

7. Savan, A.; Pflüger, E.; Voumard, P.; Schröer, A.; Paul, M.S. Modern solid lubrication: Recent developments and applications of MoS_2. *Lubr. Sci.* **2000**, *12*, 185–203. [CrossRef]

8. Spalvins, T. A review of recent advances in solid film lubrication. *J. Vac. Sci. Technol. A* **1987**, *5*, 212–219. [CrossRef]

9. National Aeronautics and Space Administration. *A Researcher's Guide to the International Space Station*; NASA: Hanover, MD, USA, 2004.

10. Brizuela, M.; Oñate, J.I.; Garmendia, I. Tribolab: An Experiment on Space Tribology, In-Orbit Data at the ISS. In Proceedings of the Proc. '13th European Space Mechanisms and Tribology Symposium–ESMATS 2009, Vienna, Austria, 23–25 September 2009.

11. Woods, T. Out of Thin Air. Available online: https://www.nasa.gov/topics/technology/features/atomic_oxygen.html. (accessed on 21 April 2020).

12. Banks, B.A.; de Groh, K.K.; Miller, S.K. *Low Earth Orbital Atomic Oxygen Interactions With Spacecraft Materials*; NASA: Hanover, MD, USA, 2004.

13. Gao, X.; Hu, M.; Sun, J.; Fu, Y.; Yang, J.; Liu, W.; Weng, L. Changes in the composition, structure and friction property of sputtered MoS_2 films by LEO environment exposure. *Appl. Surf. Sci.* **2015**, *330*, 30–38. [CrossRef]

14. Tagawa, M.; Yokota, K.; Matsumoto, K.; Suzuki, M.; Teraoka, Y.; Kitamura, A.; Belin, M.; Fontaine, J.; Martin, J.M. Space environmental effects on MoS_2 and diamond-like carbon lubricating films: Atomic oxygen-induced erosion and its effect on tribological properties. *Surf. Coat. Technol.* **2007**, *202*, 1003–1010. [CrossRef]

15. Argibay, N.; Dugger, M.T.; Krick, B.A.; Curry, J.F.; Nation, B.; Martini, A.; Strandwitz, N.C.; Babuska, T. Highly Oriented MoS_2 Coatings: Tribology and Environmental Stability. *Tribol. Lett.* **2016**, *64*, 1–9.

16. Wang, P.; Qiao, L.; Xu, J.; Li, W.; Liu, W. Erosion Mechanism of MoS_2-Based Films Exposed to Atomic Oxygen Environments. *ACS Appl. Mater. Interfaces* **2015**, *7*, 12943–12950. [CrossRef]

17. Tagawa, M.; Muromoto, M.; Hachiue, S.; Yokota, K.; Ohmae, N.; Matsumoto, K.; Suzuki, M. Hyperthermal atomic oxygen interaction with MoS_2 lubricants and relevance to space environmental effects in low earth orbit—Effects on friction coefficient and wear-life. *Tribol. Lett.* **2005**, *18*, 437–443. [CrossRef]

18. Tagawa, M.; Yokota, K.; Ochi, K.; Akiyama, M.; Matsumoto, K.; Suzuki, M. Comparison of macro and microtribological property of molybdenum disulfide film exposed to LEO space environment. *Tribol. Lett.* **2012**, *45*, 349–356. [CrossRef]

19. Serpini, E.; Rota, A.; Ballestrazzi, A.; Marchetto, D.; Gualtieri, E.; Valeri, S. The role of humidity and oxygen on MoS$_2$ thin films deposited by RF PVD magnetron sputtering. *Surf. Coat. Technol.* **2017**, *319*, 345–352. [CrossRef]

20. Sliney, H.E. Solid lubricant materials for high temperatures—A review. *Tribol. Int.* **1982**, *15*, 303–315. [CrossRef]

21. Yang, J.F.; Jiang, Y.; Hardell, J.; Prakash, B.; Fang, Q.F. Influence of service temperature on tribological characteristics of self-lubricant coatings: A review. *Front. Mater. Sci.* **2013**, *7*, 28–39. [CrossRef]

22. Wright, M.C.; Long, V.L.; McDanels, S. *The Evolution of Failure Analysis at NASA's Kennedy Space Center and the Lessons Learned*; NASA: Hanover, MD, USA, 2008.

23. Gardos, M.N. Anomalous wear behavior of MoS$_2$ films in moderate vacuum and dry nitrogen. *Tribol. Lett.* **1995**, *1*, 67–85. [CrossRef]

24. Serles, P.; Sun, H.; Colas, G.; Tam, J.; Nicholson, E.; Wang, G.; Howe, J.; Saulot, A.; Singh, C.V.; Filleter, T. Structure Dependent Wear and Shear Mechanics of Nanostructured MoS$_2$ Coatings. *Adv. Mater. Interfaces* **2020**, in press.

25. Sader, J.E.; Chon, J.W.M.; Mulvaney, P. Calibration of rectangular atomic force microscope cantilevers. *Rev. Sci. Instrum.* **1999**, *70*, 3967–3969. [CrossRef]

26. Green, C.P.; Lioe, H.; Cleveland, J.P.; Proksch, R.; Mulvaney, P.; Sader, J.E. Normal and torsional spring constants of atomic force microscope cantilevers. *Rev. Sci. Instrum.* **2004**, *75*, 1988–1996. [CrossRef]

27. Cannara, R.J.; Eglin, M.; Carpick, R.W. Lateral force calibration in atomic force microscopy: A new lateral force calibration method and general guidelines for optimization. *Rev. Sci. Instrum.* **2006**, *77*, 053701. [CrossRef]

28. Khare, H.S.; Burris, D.L. The effects of environmental water and oxygen on the temperature-dependent friction of sputtered molybdenum disulfide. *Tribol. Lett.* **2013**, *52*, 485–493. [CrossRef]

29. Kubart, T.; Polcar, T.; Kopecký, L.; Novák, R.; Nováková, D. Temperature dependence of tribological properties of MoS$_2$ and MoSe$_2$ coatings. *Surf. Coat. Technol.* **2005**, *193*, 230–233. [CrossRef]

30. Arif, T.; Yadav, S.; Colas, G.; Singh, C.V.; Filleter, T. Understanding the Independent and Interdependent Role of Water and Oxidation on the Tribology of Ultrathin Molybdenum Disulfide (MoS$_2$). *Adv. Mater. Interfaces* **2019**, *6*, 1–9. [CrossRef]

31. Levita, G.; Restuccia, P.; Righi, M.C. Graphene and MoS$_2$ interacting with water: A comparison by ab initio calculations. *Carbon* **2016**, *107*, 878–884. [CrossRef]

32. Savan, A.; Simmonds, M.C.; Huang, Y.; Constable, C.P.; Creasey, S.; Gerbig, Y.; Haefke, H.; Lewis, D.B. Effects of temperature on the chemistry and tribology of co-sputtered MoSx-Ti composite thin films. *Thin Solid Films* **2005**, *489*, 137–144. [CrossRef]

33. Khare, H.S.; Burris, D.L. Surface and subsurface contributions of oxidation and moisture to room temperature friction of molybdenum disulfide. *Tribol. Lett.* **2014**, *53*, 329–336. [CrossRef]

34. Curry, J.F.; Hinkle, A.R.; Babuska, T.F.; Wilson, M.A.; Dugger, M.T.; Krick, B.A.; Argibay, N.; Chandross, M. Atomistic Origins of Temperature-Dependent Shear Strength in 2D Materials. *ACS Appl. Nano Mater.* **2018**, *1*, 5401–5407. [CrossRef]

35. Bandaru, N.; Kumar, R.S.; Sneed, D.; Tschauner, O.; Baker, J.; Antonio, D.; Luo, S.N.; Hartmann, T.; Zhao, Y.; Venkat, R. Effect of pressure and temperature on structural stability of MoS 2. *J. Phys. Chem. C* **2014**, *118*, 3230–3235. [CrossRef]

36. Colbert, R.S.; Sawyer, G.W. Thermal dependence of the wear of molybdenum disulphide coatings. *Wear* **2010**, *269*, 719–723. [CrossRef]

37. Babuska, T.F.; Pitenis, A.A.; Jones, M.R.; Nation, B.L.; Sawyer, W.G.; Argibay, N. Temperature-Dependent Friction and Wear Behavior of PTFE and MoS$_2$. *Tribol. Lett.* **2016**, *63*, 1–7. [CrossRef]

38. Kazachenko, V.P.; Popov, V.V.; Dubravin, A.M.; Ahn, H.-S.; Chizhik, S.A. Application of phase contrast imaging atomic force microscopy to tribofilms on DLC coatings. *Wear* **2002**, *249*, 617–625.

39. Ye, J.; Kano, M.; Yasuda, Y. Determination of nanostructures and mechanical properties on the surface of molybdenum dithiocarbamate and zinc dialkyl-dithiophosphate tribochemical reacted films using atomic force microscope phase imaging technique. *J. Appl. Phys.* **2003**, *93*, 5113–5117. [CrossRef]

40. Blau, P.J. On the nature of running-in. *Tribol. Int.* **2005**, *38*, 1007–1012. [CrossRef]

41. Fleischauer, P.D. Effects of crystallite orientation on environmental stability and lubrication properties of sputtered moS. *ASLE Trans.* **1984**, *27*, 82–88. [CrossRef]

42. Moser, J.; Levy, F. Growth Mechanisms and Near-Interface Structure in Relation To Orientation of Mos2 Sputtered Thin-Films. *J. Mater. Res.* **1992**, *7*, 734–740. [CrossRef]

43. Furlan, K.P.; de Mello, J.D.B.; Klein, A.N. Self-lubricating composites containing MoS_2: A review. *Tribol. Int.* **2018**, *120*, 280–298. [CrossRef]

44. Cowen, R. The wheels come off Kepler. *Nature* **2013**, *497*, 417–418. [CrossRef]

45. Aldridge, D.; Gentilhomme, M.; Gibson, A.; Cameron, P.; Mccolgan, A. Cryogenic Motor Enhancement for the Niriss Instrument on the James Webb Space Telescope. In Proceedings of the 16th European Space Mechanisms and Tribology Symposium, Bilbao, Spain, 23–25 September 2015.